

Solvent- and Substrate-Dependent Rates of Imine Metalations by Lithium Diisopropylamide: Understanding the Mechanisms Underlying “ k_{rel} ”

Max P. Bernstein and David B. Collum*

Contribution from the Department of Chemistry, Baker Laboratory, Cornell University, Ithaca, New York 14853-1301

Received February 8, 1993

Abstract: Rate studies of the metalation of imines derived from cyclohexanone and 2-methylcyclohexanone with lithium diisopropylamide (LDA) in tetrahydrofuran (THF), *N,N,N',N'*-tetramethylethylenediamine (TMEDA), and dimethylethylamine (DMEA) mixtures are described. The *N*-isopropylimines appear to metalate via a mechanism involving deaggregation of the LDA dimer to give reactive LDA monomers without participation of additional donor solvent. TMEDA functions as an η^1 ligand in both the starting LDA dimer and the rate-determining monomeric transition state as evidenced by analogous behavior with DMEA. Comparisons of the *N*-isopropylimine metalations with previously described rate studies of the isostructural *N,N*-dimethylhydrazones provide no evidence that a $\text{Me}_2\text{N-Li}$ interaction facilitates the metalation. Metalation of imines bearing pendant Me_2N moieties on the *N*-isopropyl groups appears to proceed by either of two mechanisms. In THF and THF/hexane mixtures, the monomer-based pathway completely dominates; a $\text{Me}_2\text{N-Li}$ interaction does not appear to be important. In TMEDA/hexane mixtures and DMEA/hexane mixtures, dramatic rate accelerations are observed. Accompanying substantial changes in the mathematical forms of the rate equations suggest that the metalations proceed by double dissociation of R_3N ligands with subsequent rate-limiting metalation by the solvent-free LDA dimer. Open dimers of LDA are suggested to be the critical reactive intermediates in a mechanism shown to constitute a complex-induced proximity effect (CIPE).

Introduction

Organolithium chemistry has provided many important reagents to synthetic organic chemists. Reactive intermediates such as lithium dialkylamides, lithium enolates, and alkylolithiums are so pervasive that it would be difficult to find a complex organic synthesis that does not rely upon one or more such species.^{1,2} This prominence has caused a proliferation of crystallographic,^{3,4} spectroscopic,⁴⁻⁶ and computational^{4,7} studies that have elevated lithium far above the status of gegenion to provide an interesting and complex subdiscipline of coordination chemistry.^{2,8} Nevertheless, our understanding of organolithium reaction mechanism is still in its infancy. While the structural complexity is well established, the full mechanistic implications are not.

The unclear mechanistic picture stems, at least in part, from the limited number of detailed rate and mechanism studies.

Measured reaction orders in organolithium species document changes in aggregation state leading to the rate-limiting transition state.⁸ However, detailed investigations that address aggregation-state and solvation-state changes along the reaction coordinate are relatively rare.^{9,10} Additional confusion arises from the pervasive use and misuse of the relative rate constant, “ k_{rel} ”. One

(1) Stowell, J. C. *Carbanions in Organic Synthesis*; Wiley: New York, 1979. *Asymmetric Synthesis*; Morrison, J. D., Ed.; Academic Press: New York, 1983; Vols. 2 and 3. d'Angelo, J. *Tetrahedron* 1976, 32, 2979. Heathcock, C. H. In *Comprehensive Carbanion Chemistry*; Buncl, E., Durst, T., Ed.; Elsevier: New York, 1980; Vol. B, Chapter 4. Snieckus, V. *Chem. Rev.* 1990, 90, 879. Cox, P. J.; Simpkins, N. S. *Tetrahedron: Asymmetry* 1991, 2, 1. Caubere, P. In *Reviews of Heteroatom Chemistry*; MYU: Tokyo, 1991; Vol. 4, pp 78–139.

(2) Seebach, D. *Angew. Chem., Int. Ed. Engl.* 1988, 27, 1624. Seebach, D. In *Proceedings of the Robert A. Welch Foundation Conferences on Chemistry and Biochemistry*; Wiley: New York, 1984.

(3) Williard, P. G. In *Comprehensive Organic Synthesis*; Pergamon: New York, 1991; Vol. 1, p 1. Boche, G. *Angew. Chem., Int. Ed. Engl.* 1989, 28, 277. Setzer, W. N.; Schleyer, P. v. R. *Adv. Organomet. Chem.* 1985, 24, 354.

(4) Gregory, K.; Schleyer, P. v. R.; Snaith, R. *Adv. Inorgan. Chem.* 1991, 37, 47. Mulvey, R. E. *Chem. Soc. Rev.* 1991, 20, 167.

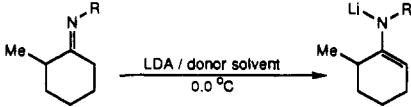
(5) Fraenkel, G.; Hsu, H.; Su, B. P. In *Lithium: Current Applications in Science, Medicine, and Technology*; Bach, R. O., Ed.; Wiley: New York, 1985; Chapter 19. Jackman, L. M.; Bortiatynski, J. In *Advances in Carbanion Chemistry*; JAI: New York, 1992; Vol. 1, pp 45–87. Moskau, D.; Bast, P.; Schmalz, D. *Angew. Chem., Int. Ed. Engl.* 1987, 26, 1212.

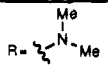
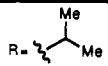
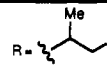
(6) Collum, D. B. *Acc. Chem. Res.* 1993, 26, 227.

(7) Leading references: Bühl, M.; van Eikema Hommes, N. J. R.; Schleyer, P. v. R.; Fleischer, U.; Kutzelnigg, W. *J. Am. Chem. Soc.* 1991, 113, 2459.

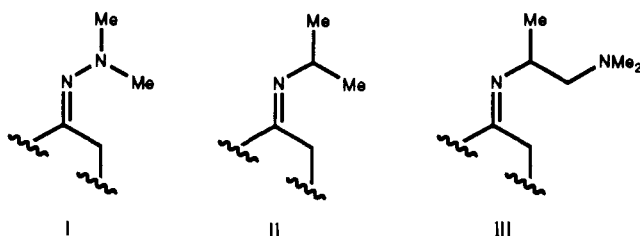
(8) General reviews: *Ions and Ion Pairs in Organic Reactions*; Szwarc, M., Ed.; Wiley: New York, 1972; Vols. 1 and 2. “Polyamine-Chelated Alkali Metal Compounds”; Langer, A. W., Jr., Ed.; American Chemical Society: Washington, DC, 1974. Szwarc, M. *Carbanions, Living Polymers, and Electron Transfer Processes*; Interscience: New York, 1968. Wardell, J. L. In *Comprehensive Organometallic Chemistry*; Wilkinson, G.; Stone, F. G. A., Abels, F. W., Eds.; Pergamon: New York, 1982. Jackman, L. M.; Lange, B. C. *Tetrahedron* 1977, 33, 2737. Wakefield, B. J. *The Chemistry of Organolithium Compounds*; Pergamon: New York, 1974, Ch. 7. *Anionic Polymerization: Kinetics, Mechanism, and Synthesis*; McGrath, J. E. Ed.; American Chemical Society: Washington, DC, 1981; Chapters 1, 2, and 29. Müller, A. H. E. In *Comprehensive Polymer Science*; Eastmond, G. C., Ledwith, A., Russo, S., Sigwalt, P., Eds.; Pergamon: New York, 1989; Vol. 3, Chapter 26. Bywater, S. *Adv. Polym. Sci.* 1965, 4, 66.

(9) Huisgen, R. In *Organometallic Chemistry*; ACS Monograph Series 147; American Chemical Society: Washington DC, 1960; pp 36–87. Wanat, R. A.; Collum, D. B. *J. Am. Chem. Soc.* 1985, 107, 2078. Depue, J. S.; Collum, D. B. *J. Am. Chem. Soc.* 1988, 110, 5524. Bartlett, P. D.; Goebel, C. V.; Weber, W. P. *J. Am. Chem. Soc.* 1969, 91, 7425. Hay, D. R.; Song, Z.; Smith, S. G. Beak, P. *J. Am. Chem. Soc.* 1988, 110, 8145. Pez, G.; Galle, J. E. *Pure Appl. Chem.* 1985, 57, 1917. Bywater, S.; Worsfold, D. J. *Can. J. Chem.* 1962, 38, 1564. Waack, R.; Doran, M. A.; Stevenson, P. E. *J. Organomet. Chem.* 1965, 3, 481. Fagley, T. F.; Klein, E. *J. Am. Chem. Soc.* 1955, 77, 786. Eastham, J. F.; Gibson, G. W. *J. Organomet. Chem.* 1966, 5, 188. Bywater, S.; Worsfold, D. J. *Can. J. Chem.* 1962, 40, 1564. Worsfold, D. J.; Bywater, S. *Can. J. Chem.* 1964, 42, 2884. Morton, M.; Fetters, L. J. *J. Polym. Sci., Part A* 1964, 2, 3311. Bywater, S.; Alexander, I. J. *J. Polym. Sci., Part A* 1968, 6, 3407. Geerts, J.; Van Beylen, M.; Smets, G. *J. Polym. Sci., Part A* 1969, 7, 2805. Davidjan, A.; Nikolae, N.; Sgonnik, V.; Belenkii, B.; Nesterov, V.; Erussalimsky, B. *Makromol. Chem.* 1976, 177, 2469. Helary, G.; Fontanille, M. *Eur. Polym. J.* 1978, 14, 345. Holm, T. *Acta Chem. Scand.* 1978, 32B, 162. O'Driscoll, K. F.; Tobolsky, A. V. *J. Polym. Sci.* 1959, 35, 259. Spirin, Yu. L.; Arest-Yakubovich, A. A.; Polyakov, D. K.; Gantmakher, A. R.; Medvedev, S. S. *J. Polym. Sci.* 1962, 58, 1181. Magnin, H.; Rodriguez, F.; Abadie, M.; Schue, F. *J. Polym. Sci., Polym. Chem. Ed.* 1977, 15, 875. Hay, J. N.; McCabe, J. F.; Robb, J. C. *J. Chem. Soc., Faraday Trans.* 1972, 68, 1. Hay, J. N.; McCabe, J. F.; Robb, J. C. *J. Chem. Soc., Faraday Trans.* 1972, 68, 1227. See also ref 10.

Table I. Relative Rate Constants for the LDA-Mediated Metallation of 2-Methylcyclohexanone Imine Derivatives


solvent	R = 	R = 	R = 
THF	18	1.3	1.8
Me ₂ NCH ₂ CH ₂ NMe ₂	22	2.3	93
Me ₂ NCH ₂ CH ₃	23	1.0	28

can readily measure the rates for a series of related reactions without recourse to detailed kinetic analyses. Alternatively, selectivities provide a less direct, but often more expedient, source of *relative* rate data. We offer Table I as typical of what one might find in the literature. Given the relative rate data, it is then the burden of the experimentalist to discern any patterns and trends of mechanistic importance. While this approach may provide tractable results for some simple organic reactions, it is inadequate to unravel the mechanistic complexities found in organolithium chemistry.



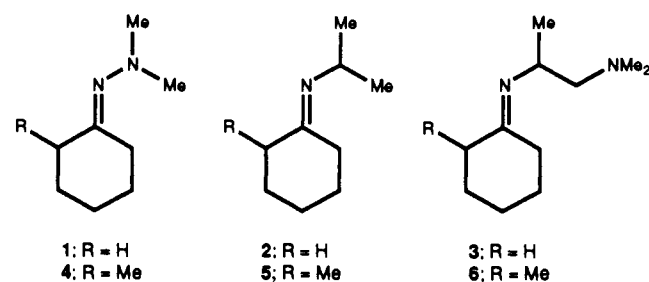
This paper presents detailed rate studies of imine metalations by lithium diisopropylamide (LDA) in three solvents: *N,N,N',N'*-tetramethylethylenediamine (TMEDA), tetrahydrofuran (THF), and dimethylethylamine (DMEA). Our primary goal was to determine whether the Me₂N moieties of *N,N*-dimethylhydrazones (i) or imines of type iii assist the proton abstraction by LDA, a phenomenon referred to as the "complex-induced proximity effect" (CIPE).¹¹⁻¹⁵ *Of more general importance, however, is the demonstration that solvent- and substrate-dependent rate changes ("k_{rel}") can only be fully understood in the context of the rate equations.* The specific results and conclusions we wish to underscore are as follows: (1) *N,N*-Dimethylhydrazones (i) and the isostructural *N*-isopropylimines (ii) metalate by analogous mechanisms involving transient monomers (Scheme I). The mathematically indistinguishable rate equations argue against a potentially favorable Me₂N–lithium interaction in the hydrazone metalation transition state. (2) Imines of type iii bearing a remote Me₂N ligand appear to react via transient monomers in the presence of THF (Scheme I) or

via solvent-free dimers in TMEDA/hexane and DMEA/hexane mixtures (Scheme II). The large rate accelerations associated with the emergence of the dimer-based metalation pathway depend critically upon the facile dissociation of *two* ligands. (3) The rate studies provide strong support for recent suggestions that TMEDA-mediated rate accelerations may stem from weak metal–ligand interactions and that the role of TMEDA is generally not well understood. (4) A simple, semiquantitative method for determining the relative binding affinities of standard donor solvents toward LDA allows us to dissect solvent-dependent rate changes into ground-state and transition-state contributions. (5) Mechanistic relationships detected through detailed analysis of the rate equations suggest new criteria for invoking a CIPE.¹⁶

Results

Table I provides normalized relative rate constants for a variety of structurally related imines derived from 2-methylcyclohexanone simply to illustrate trends within an isostructural series. Because of the wide range in the rates, both the largest and smallest values should be viewed as approximate. We also find that the relative rates of the methylated cyclohexanone derivatives do not always parallel those of the nonmethylated cases described below. Methylation generally suppresses the metalation rates in TMEDA more so than in THF.

In this section we will describe the protocol for determining rate equations for metalations of imines of types i–iii in THF, DMEA (Me₂NCH₂CH₃), and TMEDA. All nine imine–solvent combinations can be described by rate equations of two general mathematical forms (eqs 1 and 2). The results are summarized as a tabulation of calculated reaction orders and kinetic isotope effects (Table II). Since the IR spectroscopic method used to follow the kinetics offers a limited window of reaction rates (see Table I),¹⁰ we found it necessary to modulate the rates to permit the determination of complete rate equations. Reaction rates have been adjusted using substrates (1–6) prepared from cyclohexanone derivatives with minor changes in several parameters. The temperature is maintained at either 20 °C, or, for rapid metalations, at 0 °C. Inclusion of 2-methyl substituents and perdeuteration of the 2 and 6 positions of the cyclohexanone portion also slow the metalation rates. Imine substrates (in decreasing order of reactivity) derive from cyclohexanone, 2,2,6,6-tetradeuteriocyclohexanone, 2-methylcyclohexanone, or 2,6,6-trideuterio-2-methylcyclohexanone.¹⁷



$$d[\text{imine}]/dt = k'[\text{imine}][\text{LDA}_T]^{1/2}[\text{TMEDA}]^0 \quad (1)$$

$$d[\text{imine}]/dt = k''[\text{imine}][\text{LDA}_T][\text{TMEDA}]^{-2} \quad (2)$$

There are two essential features of the rate data summarized in Table II that should be understood at the onset. First, the rate equations for a given solvent–imine combination are determined at a single temperature using a single substrate; the reaction parameters used to modulate the rates *do not vary within an empirically determined rate equation*. Consequently, each rate

(10) Galiano-Roth, A. S.; Collum, D. B. *J. Am. Chem. Soc.* **1989**, *111*, 6772. Bernstein, M. P.; Romesberg, F. E.; Fuller, D. J.; Harrison, A. T.; Collum, D. B.; Liu, Q.-Y.; Williard, P. G. *J. Am. Chem. Soc.* **1992**, *114*, 5100.

(11) Beak, P.; Meyers, A. I. *Acc. Chem. Res.* **1986**, *19*, 356.

(12) Hay, D. R.; Song, Z.; Smith, S. G.; Beak, P. *J. Am. Chem. Soc.* **1988**, *110*, 8145. Gronert, S.; Streitwieser, A., Jr. *J. Am. Chem. Soc.* **1988**, *110*, 2843. Chen, X.; Hortelano, E. R.; Eliel, E. L.; Frye, S. V. *J. Am. Chem. Soc.* **1992**, *114*, 1778. Das, G.; Thornton, E. R. *J. Am. Chem. Soc.* **1990**, *112*, 5360. van Eikema Hommes, N. J. R.; Schleyer, P. v. R. *Angew. Chem., Int. Ed. Engl.* **1992**, *31*, 755. Jackman, L. M.; Petrei, M. M.; Smith, D. *J. Am. Chem. Soc.* **1991**, *113*, 3451. Retz, M. T.; Raguse, B.; Marth, C. F.; Hügel, H. M.; Bach, T.; Fox, D. N. A. *Tetrahedron* **1992**, *48*, 5731.

(13) Klumpp, G. W. *Recl. Trav. Chim. Pays-Bas* **1986**, *105*, 1.

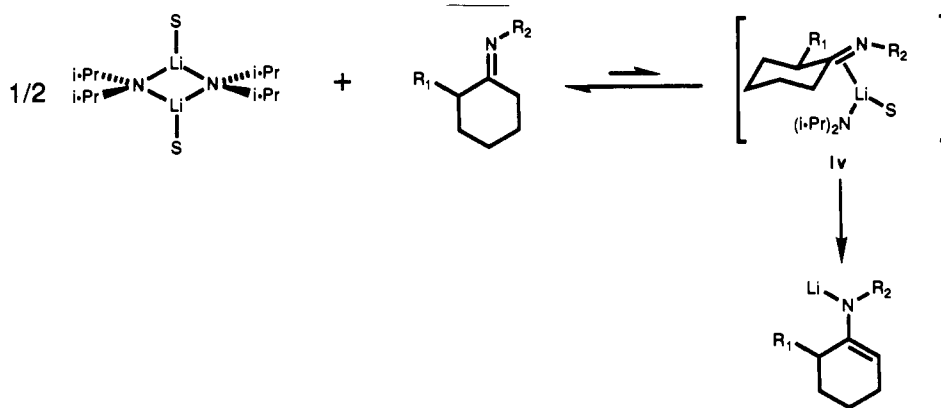
(14) Cram, D. J.; Wilson, D. R. *J. Am. Chem. Soc.* **1963**, *85*, 1245.

(15) For an excellent review of the literature on chelation-directed chemistry prior to 1980, see: Bartlett, P. A. *Tetrahedron* **1980**, *36*, 2. See also: Retz, M. T.; *Angew. Chem., Int. Ed. Engl.* **1984**, *30*, 1531 and citations in ref 12.

(16) Some of these results have been communicated previously: Bernstein, M. P.; Collum, D. B. *J. Am. Chem. Soc.* **1993**, *115*, 789.

(17) Peet, N. P. *J. Labeled Compd.* **1973**, *9*, 721.

Scheme I



Scheme II

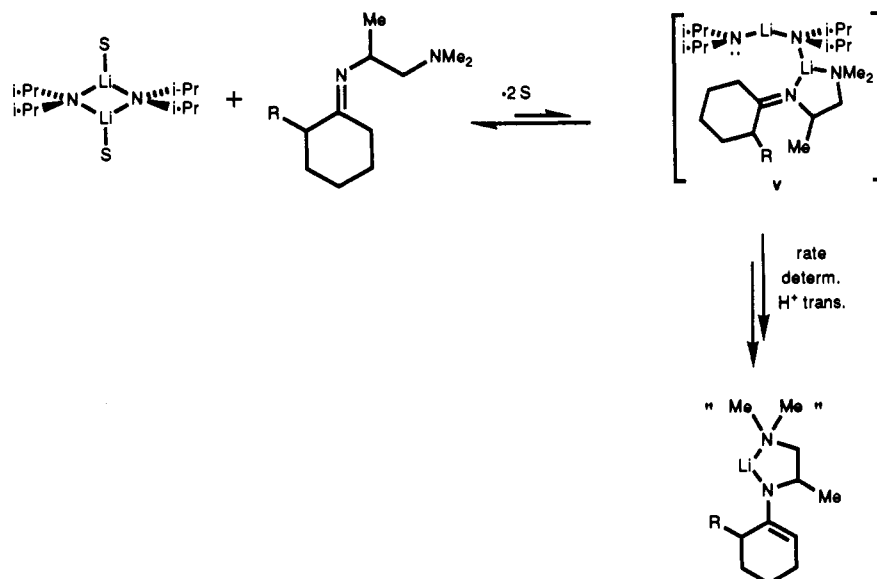


Table II. Reaction Orders and Kinetic Isotope Effects for LDA-Mediated Imine Metalations^a

substrate	solvent	temp, °C	THF order ^b	LDA order	k_H/k_D
2	THF	20 ± 0.1	0 ^b	0.49 ± 0.02	11.2 ± 2.0
	TMEDA	20 ± 0.1	0	0.51 ± 0.01	6.2 ± 1.2
	DMEA	20 ± 0.1	0	0.54 ± 0.04	7.7 ± 1.0
4	THF	0.0 ± 0.5	0	0.45 ± 0.01	6.4 ± 0.6
	TMEDA	0.0 ± 0.5	0	0.55 ± 0.05	8.3 ± 1.2
	DMEA	0.0 ± 0.5	0	0.47 ± 0.01	6.9 ± 1.8
6	THF	0.0 ± 0.5	0	0.55 ± 0.03	>5 ^c
	TMEDA	0.0 ± 0.5	-2.02 ± 0.01	1.06 ± 0.03	2.0 ± 0.1
	DMEA	0.0 ± 0.5	-2.20 ± 0.01	0.96 ± 0.03	2.3 ± 0.1

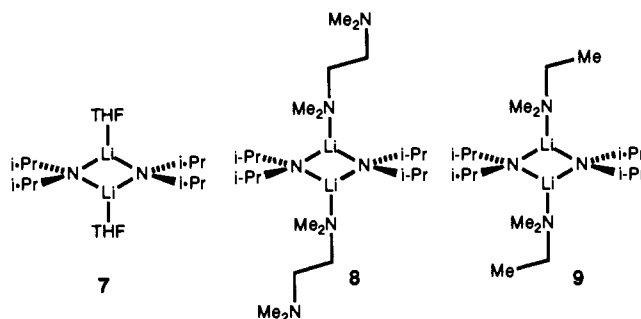
^a Rate studies of the *N,N*-dimethylhydrazones were described previously. ^b The zero orders were readily determined by visual inspection (see Figures 3 and 4, for example) rather than by numerical fit. ^c Extremely low metallation rates for **6-d₃** in THF render the isotope effect approximate.

equation is a self-consistent kinetic study. Second, in those cases where we compare rate equations of differing substitution (H vs Me) or temperature (0 vs 20 °C), we have cross-checked the results with several isostructural and isothermal comparisons. We find no direct evidence that these subtle variations used to adjust the rates cause significant mechanistic changes.¹⁸

Starting Materials and Structures. The LDA used in the kinetic analyses was generated from diisopropylamine and *n*-BuLi and multiply recrystallized.^{19,20} A combination of one- and two-

(18) We add, however, that the metallations of imine **3** in THF are surprisingly rapid. Omission of the 2-methyl substituent may cause contributions from the open-dimer-based pathway to become significant. Further studies are in progress.

dimensional NMR methods reveals the structure of LDA in THF, TMEDA, and DMEA solution to be 7–9, respectively. The cyclic dimer assignments derive from ⁶Li–¹⁵N double labeling studies⁶ in conjunction with ¹⁵N zero-quantum NMR spectroscopy.^{10,21,22} The solvation-state assignments are based upon less direct evidence summarized elsewhere,⁶ but are fairly secure nonetheless. Similarly, assignment of nonchelated (η^1) TMEDA ligands in **8** derives from strong indirect evidence described previously;¹⁰ the kinetic studies described below provide additional support.



(19) Kim, Y.-J.; Bernstein, M. P.; Galiano-Roth, A. S.; Romesberg, F. E.; Williard, P. G.; Fuller, D. J.; Harrison, A. T.; Collum, D. B. *J. Org. Chem.* **1991**, *56*, 4435.

(20) Rate constants obtained using purified LDA prepared from crystalline (halide-free) ethyllithium or commercial *n*-BuLi/hexane are indistinguishable.

(21) Gilchrist, J. H.; Collum, D. B. *J. Am. Chem. Soc.* **1992**, *114*, 794.

(22) We thank Brett Lucht for recording the ¹⁵N zero-quantum NMR spectrum of [⁶Li,¹⁵N]LDA in DMEA.

Hydrazones and imines 1–6 used in the kinetic analyses were prepared by modifications of standard literature procedures. The 2,6,6-tri- and 2,2,6,6-tetradeuterated analogues were prepared from 2,6,6-trideuterio-2-methylcyclohexanone and 2,2,6,6-tetradeuteriocyclohexanone (respectively), special precautions being taken to ensure retention of the isotopic enrichment. The deuteration was >97%, as shown by ^1H NMR spectroscopy.

Imine Metalation Kinetics: General. Previous studies of the lithiation of *N,N*-dimethylhydrazone 4 by LDA in THF, TMEDA, and DMEA provide foundations for studying the metalation of imines.¹⁰ Metalation rates were determined by monitoring the loss of the C=N stretch of the starting imine (1656–1660 cm^{-1}) using the continuous-flow IR spectroscopic apparatus described previously.¹⁰ Helium rather than the more standard inert gases minimized a degassing problem specific to the flow system. Rate constants determined by monitoring product formation (1590–1600 cm^{-1}) are comparable within experimental error ($\pm 10\%$) to those determined by monitoring loss of starting material. Neither the intensities nor positions of the C=N absorbances of the imines are measurably perturbed by added LDA, confirming¹⁰ that LDA–imine complexes are not detectable.²³ Pseudo-first-order conditions were established with LDA at normal concentrations (typically 0.13 M) by restricting the imine concentrations to 0.004 M. The donor solvent concentrations were maintained at high, yet adjustable, concentrations (with indicated cosolvents) to determine the mathematical form of the solvent dependencies. Imines 6 and 6-*d*₃ were prepared as an inseparable mixture of two racemic diastereomers. Although the two diastereomers could metalate at different rates, plots of absorbance vs time show no evidence of differential reactivities.

The reaction orders and isotope effects for all imine metalations are summarized in Table II. The results from two previous studies of *N,N*-dimethylhydrazone metalations¹⁰ are included in Table II for forthcoming comparisons and discussions. The methods used to determine the reaction orders are described below using representative plots for illustration. In general, the orders were determined from the appropriate least-squares analyses (see below) using 6–13 independently measured rate constants. The remaining plots and tables of rate constants are included in the supplementary material.

Imine Metalation Kinetics: Reaction Orders in Imine. The metalations of all imines in all solvents followed clean first-order behavior in imine and typically were monitored to ≥ 6 half-lives. The rate constants were determined through nonlinear least-squares fits to eq 3. The imine orders were checked by showing that the observed rate constants are independent of the initial imine concentration. In principle, low concentrations of mixed aggregate, homonuclear aggregate, or any unseen byproduct of the reaction (such as diisopropylamine²⁴ or solvent metalation products^{25,26}) could measurably influence the rate of the metalation. Very simple control experiments excluded percent-conversion-dependent rate effects. Upon completion of a number of the kinetic runs, the spectral base line was reestablished, an additional aliquot of imine was added, and the pseudo-first-order rate constant for the disappearance of imine was determined. Differences in the measured rate constants for the first and second aliquots were always equal within experimental error ($\pm 10\%$). The isotope effects were determined by comparing the rate

(23) For leading references to detectable organolithium–substrate pre-complexation, see ref 13. For theoretical studies of substrate pre-complexation, see: Bachrach, S. M.; Ritchie, J. P. *J. Am. Chem. Soc.* **1989**, *111*, 3134 and references cited therein.

(24) Spectroscopic studies reveal that diisopropylamine does not measurably bind to LDA in hexane at -95 or 20°C (ref 10).

(25) Melchior, M. T.; Klemann, L. P.; Whitney, T. A.; Langer, A. W., Jr. *Polym. Prepr. (Am. Chem. Soc., Div. Polym. Chem.)* **1972**, *13*, 649. Koehler, F. H.; Hertkorn, N.; Bluemel, J. *Chem. Ber.* **1987**, *120*, 2081. Kopka, I. E.; Fataftah, Z. A.; Rathke, M. W. *J. Org. Chem.* **1987**, *52*, 448.

(26) Bates, R. B.; Kroposki, L. M.; Potter, D. E. *J. Org. Chem.* **1970**, *37*, 560. Stanetty, P.; Koller, H.; Mihovilovic, M. *J. Org. Chem.* **1992**, *57*, 6833.

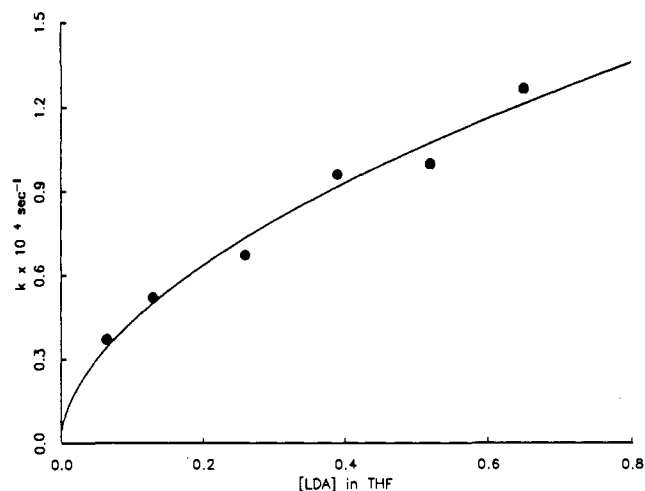


Figure 1. Plot of k_{obsd} versus [LDA] in neat THF for the metalation of imine 2-*d*₄ (0.004 M) at $0.0 \pm 0.5^\circ\text{C}$. The curve depicts the result of an unweighted nonlinear least-squares fit to eq 4 ($n = 0.49 \pm 0.02$).

constants derived from unlabeled substrates with those derived from the 2,6,6-tri- and 2,2,6,6-tetradeuterio analogues.

$$\text{abs}_t = (\text{abs}_0 - \text{abs}_\infty)e^{-kt} + \text{abs}_\infty \quad (3)$$

Imine Metalation Kinetics: Reaction Orders in LDA. Figure 1 illustrates the dependence of the pseudo-first-order rate constants for metalation of 2-*d*₄ on the LDA concentration (0.065–0.39 M) in neat THF. The downward curvature in Figure 1 is characteristic of a fractional order. A nonlinear least-squares fit to eq 4 provides a calculated LDA order of 0.49 ± 0.02 , consistent with a spectroscopically invisible dimer–monomer preequilibrium. In contrast, imines of type iii in either TMEDA/hexane mixtures or DMEA/hexane mixtures afford distinctly different results.²⁷

$$k_{\text{obsd}} = k[\text{LDA}]^n \quad (4)$$

Initial studies of the metalations of 3 and 3-*d*₄ in neat TMEDA revealed rates that were too high to monitor within the restrictions of the continuous-flow IR cell, clearly demonstrating that the pendant Me_2N facilitates the metalation. Fortunately, reduced metalation rates of the methylated derivatives 6 and 6-*d*₃ allowed for precise rate measurements. Figure 2 illustrates the dependence of the pseudo-first-order rate constants for metalation of 6 in neat TMEDA on the LDA concentration (0.065–0.39 M). The curve in Figure 2 corresponds to a *nonlinear* least-squares fit to equation 4. The linearity ($n = 1.06 \pm 0.03$) reveals the first-order dependence on the LDA concentration and indicates that the LDA dimer reacts *without prior deaggregation*.

Imine Metalation Kinetics: Reaction Orders in Donor Solvent. Figure 3 illustrates the dependence of the pseudo-first-order rate

(27) We were prompted by communications with Professor Andrew Streitwieser and Jim Krom (University of California—Berkeley) to elaborate on the possibility that the metalations might proceed by a combination of monomer-dependent and dimer-dependent pathways. In this instance, the parallel half-order and first-order pathways would cause a significant deviation of the calculated LDA orders (Table II) from the optimal values of 0.50 and 1.00, respectively. Moreover, data analysis according to the binomial expression

$$k_{\text{obsd}} = k[\text{LDA}]^{0.5} + k[\text{LDA}]$$

would afford a significantly improved fit relative to the analogous treatments assuming a single pathway. However, in all cases this alternative binomial treatment provides contributions from a second pathway that are neither large nor statistically significant (one-tailed *F*-test; 95% confidence level). We thank Streitwieser and Krom for an extremely diligent and thoughtful reading of the manuscript. We thank F. E. Romesberg (Cornell) for enlightening discussions and assistance while reevaluating the statistical methods.

(28) The mixture of oligomers of solvent-free LDA precludes a rigorous treatment. We restrict the model to one molecule of TMEDA coordinated per lithium (enforcing $n = 2$) and report the values of K_{eq} without units.

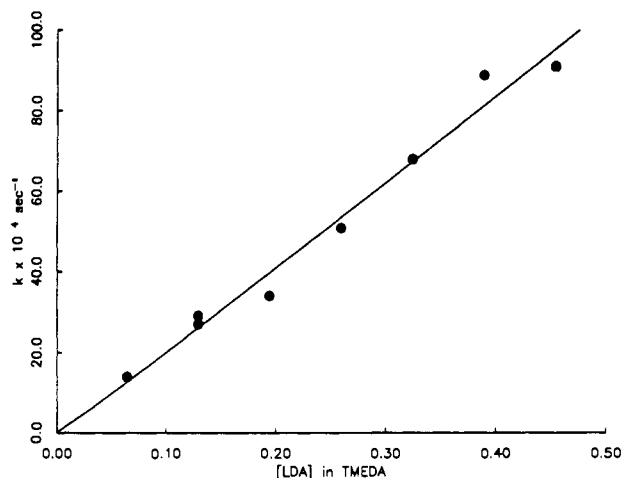


Figure 2. Plot of k_{obsd} versus [LDA] in neat TMEDA for the metalation of imine **6** (0.004 M) at 0.0 ± 0.5 °C. The curve depicts the result of an unweighted, nonlinear least-squares fit to the general equation, eq 4 ($n = 1.06 \pm 0.03$).

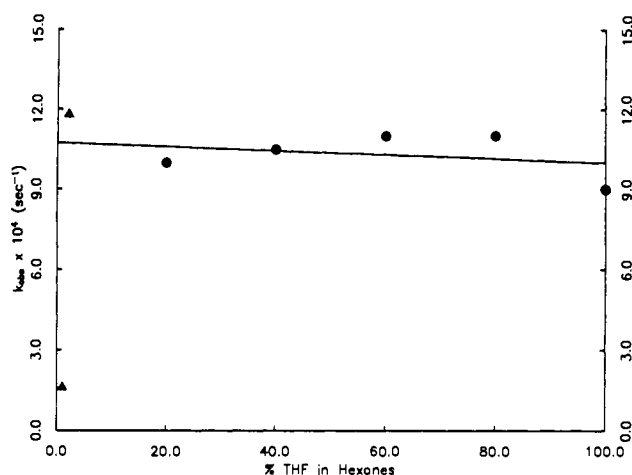


Figure 3. Plot of k_{obsd} versus [THF] in hexane cosolvent for the metalation of imine **2-d₄** (0.004 M) by LDA (0.13 M) at 0.0 ± 0.5 °C. The curve depicts the result of an unweighted linear least-squares fit. The rate constants designated by triangles (\blacktriangle) were not included in the fit.

constants for metalation of **2-d₄** plotted as a function of the [THF] in hexane cosolvent. The independence of the rate constants on the [THF] implicates a metalation mechanism involving equivalent per-lithium solvation number in the ground state and rate-limiting transition state. The absence of a substantial falloff in rate even at very low THF concentrations (2 equiv) shows a highly favorable solvation of LDA by THF. This contrasts with the results observed for the metalation of **2-d₄** by LDA in TMEDA/hexane mixtures (Figure 4). A zero-order TMEDA dependence is observed at high (>25% by volume) [TMEDA] akin to that observed for THF. However, the fall-off region occurring between 0 and 25% by volume TMEDA reflects a very soft solvent-dependent equilibrium. This [TMEDA]-dependent saturation kinetics was shown by previous studies¹⁰ to correlate quantitatively with the conversion of unsolvated LDA oligomers to disolvated dimer **8** requiring surprisingly high TMEDA concentrations (see Scheme III). Thus, the data depicted in Figures 3 and 4 reaffirm previous conclusions that TMEDA is a relatively poor ligand for LDA.¹⁰

There is no analytical rate equation to describe the saturation behavior in Figure 4 due to the uncertainty in the mechanism of the slow (but measurable) metalation by the unsolvated LDA oligomers (Scheme III). Yet, eqs 5 and 6 represent a reasonable approximation (see supplementary material). The constant, k_1 , reflects the minor contribution of solvent-free LDA to the

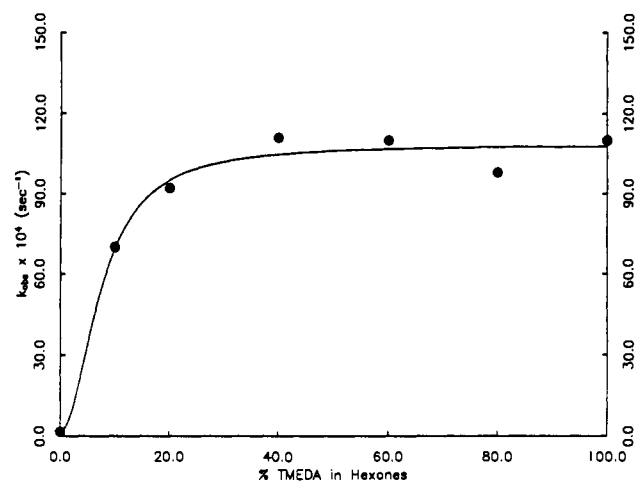
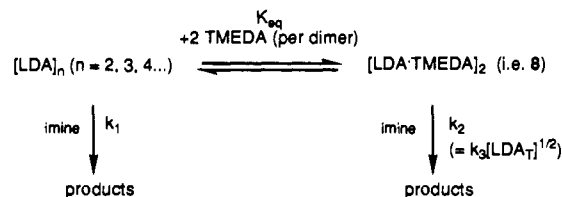


Figure 4. Plot of k_{obsd} versus [TMEDA] in hexane cosolvent for the metalation of imine **2-d₄** (0.004 M) by LDA (0.13 M) at 0.0 ± 0.5 °C. The curve depicts the result of an unweighted nonlinear least-squares fit to eq 7. The values of the adjustable parameters were as follows: $K_{\text{eq}} = 1.6 \pm 0.6$, $k_2 = 108 \pm 30 \times 10^{-4} \text{ s}^{-1}$, and $k_1 = 4.0 \pm 0.9 \times 10^{-4} \text{ s}^{-1}$ (see Table II). The falloff in rates below 25% by volume TMEDA was shown previously to coincide with the desolvation of the LDA.¹¹

Scheme III



metalation rate (see Scheme III) and defines the y-intercept. Although this contribution would not formally be constant, the value is of a magnitude comparable to experimental error and is included merely to define the minor nonzero y-intercept. Under pseudo-first-order conditions at fixed LDA concentration, eq 6 reduces to eq 7. In the limit of high TMEDA concentration, the observed pseudo-first-order rate constant becomes [TMEDA]-independent, consistent with experiment. In the event, the curve in Figure 4 corresponds to a nonlinear least-squares fit to eq 7 with adjustable parameters $K_{\text{eq}} = 1.6 \pm 0.6$, $k_1 = 0.4 \pm 0.1 \times 10^{-3} \text{ s}^{-1}$, and $k_2 = 11 \pm 3 \times 10^{-3} \text{ s}^{-1}$. The calculated value of K_{eq} , although an approximation, should be substrate-independent.²⁸ Indeed, the value for K_{eq} determined from imine metalations agrees well with the value of 1.3 ± 0.3 determined from hydrazone metalations.¹⁰

$$d[\text{imine}]/dt = k_{\text{obsd}}[\text{imine}] \quad (5)$$

$$k_{\text{obsd}} = \frac{k_3 K_{\text{eq}} [\text{LDA-T}]^{1/2} [\text{TMEDA}]}{1 + K_{\text{eq}} [\text{TMEDA}]} + k_1 \quad (6)$$

$$k_{\text{obsd}} = \frac{k_2 K_{\text{eq}} [\text{TMEDA}]}{1 + K_{\text{eq}} [\text{TMEDA}]} + k_1 \quad (7)$$

$$\text{(such that } k_2 = k_3 K_{\text{eq}}''^{1/2} [\text{LDA-T}]^{1/2}\text{)}$$

In stark contrast with all previously described cases, rate constants for metalation of **6** by LDA in TMEDA/hexane mixtures rise exponentially with *decreasing* TMEDA concentration. The rate data in Figure 5 were fit to the expression in eq 8, revealing an *inverse second-order dependence on [TMEDA]*. The constant, k'' , appended to eq 8 corresponds to the nonzero rate constant for metalation at infinite TMEDA concentration where the solvent-independent (and relatively insignificant)

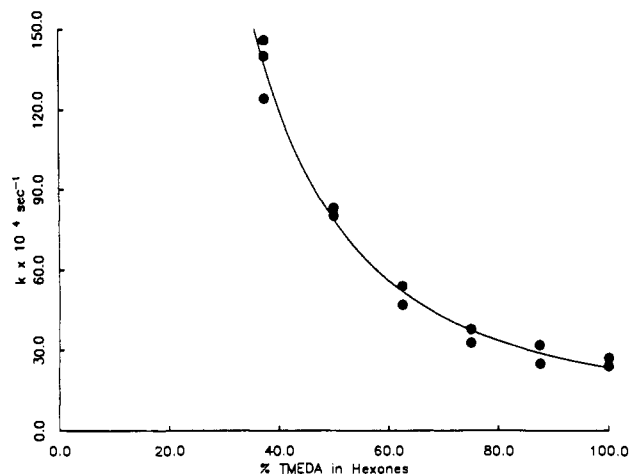


Figure 5. Plot of k_{obsd} versus [TMEDA] in hexane cosolvent for the metalation of imine **6** (0.004 M) by LDA (0.13 M) at 0.0 ± 0.5 °C. The curve depicts the result of an unweighted least-squares fit to eq 8. The adjustable parameter, n , corresponds to the order in TMEDA ($n = -2.02 \pm 0.01$). The parameter k_1 corresponds to the observed rate constant expected for the metalation via monomers ($k'' = 5.2 \pm 1.7 \times 10^{-4} \text{ s}^{-1}$).

Scheme IV



monomer-based mechanism (Scheme I) would become dominant.²⁹ The role of solvent dissociation was further supported by the observation that addition of 2.5% by volume THF strongly inhibits metalations of **3** and **6** in neat DMEA or TMEDA. This is consistent with the superior ligating capacity of THF relative to either DMEA or TMEDA (see below).

$$k_{\text{obsd}} = k'[\text{TMEDA}]^n + k'' \quad (8)$$

Determination of Relative Solvent Binding Constants. Monitoring metalation rates in a mixture of two donor solvents over the entire solvent mole fraction range can provide insight into the role of solvation. Consider, for example, the equilibrium in Scheme IV, the artist's rendition of plots of k_{obsd} vs donor solvent mole fraction depicted in Figure 6, and the simple thermochemical picture in Figure 7. In the limit of either neat S_1 or neat S_2 , the two limiting observable species are vi and vii, respectively. Qualitatively we note that a relatively low concentration of the superior donor solvent should be sufficient to shift the equilibrium. Consequently, the inflection point and fall-off region will necessarily reside closer to the y -axis corresponding to the neat inferior donor solvent. If one subscribes to the notion that strong donor solvents afford kinetically reactive species,³⁰ the y -intercept nearest the inflection point will correspond to the lower of the two intercepts (curve A in Figure 6). If, on the other hand, the solvent donicity and kinetic reactivity correlate inversely, then the behavior typified by curve B in Figure 6 will result.

(29) In principle, the calculated value of k'' ($5.2 \pm 1.7 \times 10^{-4} \text{ s}^{-1}$) might be expected to correlate with the measured value of k_{obsd} of $0.66 \pm 0.17 \times 10^{-4} \text{ s}^{-1}$ for metalation of *N*-isopropylimine **5** in neat TMEDA. The analogous plot of k_{obsd} vs solvent composition in DMEA hexane mixtures affords $240 \pm 48 \times 10^{-4} \text{ s}^{-1}$ for k'' compared to the value of $29 \pm 0.3 \times 10^{-4} \text{ s}^{-1}$ for k_{obsd} observed in metalations in **5** in neat DMEA. Both correlations probably suffer from the inaccuracy caused by extrapolations of a nonlinear function to infinity.

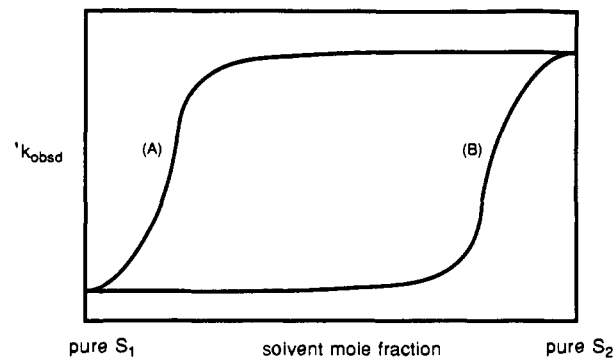


Figure 6.

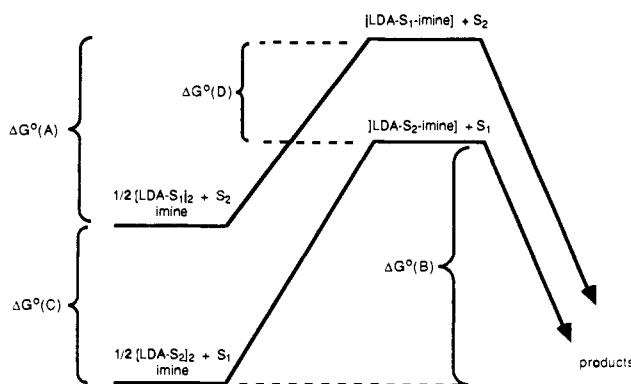


Figure 7.

The utility of this simple strategy for investigating LDA solvation is that it offers more quantitative insight as well. The two y -intercepts correspond to $k_{\text{obsd}}(\text{S}_1)$ and $k_{\text{obsd}}(\text{S}_2)$ (i.e. " k_{rel} "), providing the free energies of activation ($\Delta G^\circ(\text{A})$ and $\Delta G^\circ(\text{B})$, Figure 7). The function showing a sigmoidal fall-off region is described by eq 9. Substituting for $[\text{S}_1]$ in terms of $[\text{S}_2]$ in eq 9, we obtain an algebraic expression (eq 10) that allows the binding constant, $K_{\text{eq}}(\text{S}_2/\text{S}_1)$, to be determined by simple numerical methods. (The constants a and b adjust for the molar volumes; see supplementary material.) The calculated value of $K_{\text{eq}}(\text{S}_2/\text{S}_1)$ provides a measure of the difference in free energies of the two ground-state structures vi and vii ($\Delta G^\circ(\text{C})$, Figure 7). The estimated activation free energies and relative ground-state free energies, when taken together, provide the difference in the transition-state energies (i.e. $\Delta G^\circ(\text{D})$) and complete the albeit highly simplified thermochemical picture in Figure 7.

$$k_{\text{obsd}} = \{k_1[\text{S}_1]^2 + k_2K_{\text{eq}}[\text{S}_2]^2\} / \{[\text{S}_1]^2 + K_{\text{eq}}[\text{S}_2]^2\} \quad (9)$$

(such that $K_{\text{eq}} = K_{\text{eq}}(\text{S}_1/\text{S}_2)$, $k_1 = k_{\text{obsd}}(\text{S}_1)$,

and $k_2 = k_{\text{obsd}}(\text{S}_2)$)

$$k_{\text{obsd}} = \{k_1[\text{S}_1]^2 + k_2K_{\text{eq}}(a-b[\text{S}_1])^2\} / \{[\text{S}_1]^2 + K_{\text{eq}}(a-b[\text{S}_1])^2\}$$

(such that $a = [\text{S}_2]_{\text{neat}}$ and $b = [\text{S}_2]_{\text{neat}}/[\text{S}_1]_{\text{neat}}$) (10)

Before considering the experimental results, it is important to understand the assumptions and approximations that render the

(30) There are a number of reports where ostensibly weaker solvent-lithium interactions lead to increased overall reaction rates: Appar, M.; Barreille, M. *Tetrahedron* **1978**, *34*, 1541. Loupy, A.; Seyden-Penne, J. *Tetrahedron* **1980**, *36*, 1937. Reich, H. J.; Green, D. P.; Phillips, N. H. *J. Am. Chem. Soc.* **1989**, *111*, 3444. Loupy, A.; Seyden-Penne, J.; Tchoubar, B. *Tetrahedron Lett.* **1976**, 1677. Bywater, S.; Worsfold, D. J. *Can. J. Chem.* **1962**, *40*, 1564. Kündig, E. P.; Desobry, V.; Simmons, D. P.; Wenger, E. *J. Am. Chem. Soc.* **1989**, *111*, 1804. Reich, H. J.; Phillips, N. H.; Reich, I. L. *J. Am. Chem. Soc.* **1985**, *107*, 4101. Klumpp, G. W. *Recl. Trav. Chim. Pays-Bas* **1986**, *105*, 1. Galiano-Roth, A. S.; Collum, D. B. *J. Am. Chem. Soc.* **1989**, *111*, 6772.

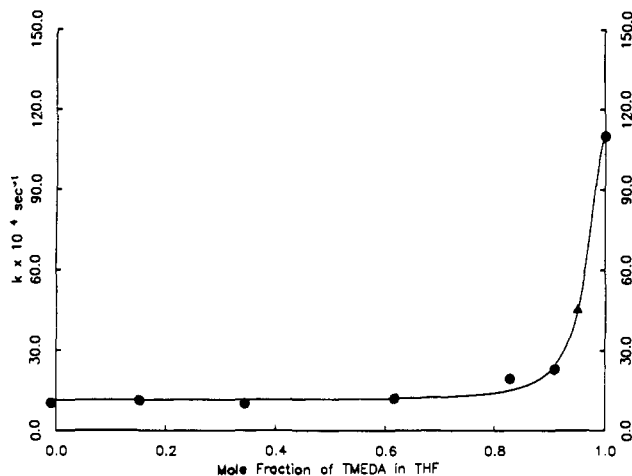


Figure 8. Pseudo-first-order rate constants for the metalation of imine **2-d₄** (0.004 M) by LDA (0.13 M) as a function of TMEDA and THF composition. The units on the *x*-axis correspond to solvent mole fraction $[TMEDA]/([TMEDA] + [THF])$. An unweighted least-squares fit to eq 10 affords $K_{eq}(THF/TMEDA) = 75 \pm 2$. The rate constant designated by a triangle (\blacktriangle) was not recorded under fully pseudo-first-order conditions and was not included in the fit.

model only semiquantitative. (1) If the magnitudes of the *y*-intercepts are fortuitously equivalent (as found for metalations of **4** in THF and TMEDA),¹⁰ the consequent failure to observe a solvent-composition-dependent change in rate renders the method inoperative. (2) In the event that the metalation mechanisms operative in the near donor solvents have nonzero reaction orders in donor solvent, $k_{obsd}(S_1)$ and $k_{obsd}(S_2)$ would be dependent upon the solvent concentration. In turn, the mathematical description would become substantially more complex than implied by eq 10. Fortunately, most of the imine and hydrazone metalations are zero-order in donor solvent concentration. (3) The precise shape of the sigmoid and the accuracy of the value of $K_{eq}(S_2/S_1)$ depend on the assumed solvation states of vi and vii that are based upon compelling (yet still indirect) evidence for the cases described below.⁶ Should one or both of the solvation-state assignments be incorrect, the mathematical form of eq 10 would be incorrect. (4) The model does not account for the very real possibility of kinetically important mixed solvated dimers. The contribution of mixed solvates is predicted to be maximized near the inflection point of the binary model.³¹ Although we do not detect substantial evidence of mixed solvates in the examples described below, rate studies of hydrazone metalations in tetrahydrofuran/2,5-dimethyltetrahydrofuran mixtures have revealed evidence of kinetically important mixed solvates.¹⁰ (5) When measuring pseudo-first-order rate constants using solvent mixtures, it is important that both solvents are in excess (≥ 10 equiv per Li) so as not to include substantial distortions in the free solvent concentration. As we shall see, the fall-off region is often barely visible under this restriction.

Figure 8 shows the measured pseudo-first-order rate constants for the metalation of imine **2-d₄** plotted as a function of TMEDA mole fraction in THF. Fitting of the data to eq 10 ($S_1 = TMEDA$ and $S_2 = THF$) affords $K_{eq}(THF/TMEDA) = 75 \pm 2$ (favoring the THF solvate) and $k_{obsd}(TMEDA)/k_{obsd}(THF) = 12$.³² This affords a ground-state energy difference, $\Delta G^\circ(C)$, of 2.4 ± 0.1 kcal/mol and a transition-state energy difference, $\Delta G^\circ(D)$, of 1.0 ± 0.04 kcal/mol. Accordingly, we draw two interesting conclusions: (1) TMEDA is indeed inferior to THF as a ligand for dimeric LDA, and (2) the origin of the rate acceleration

(31) The mixed solvate would be optimal precisely at the inflection points of Figure 6 if the two ligand substitutions were energetically equivalent.

(32) One may note that the values of k_{rel} gleaned from Figures 8, 9, and 11 do not correlate with the values of the methylated derivatives in Table I as noted at the start of Results.

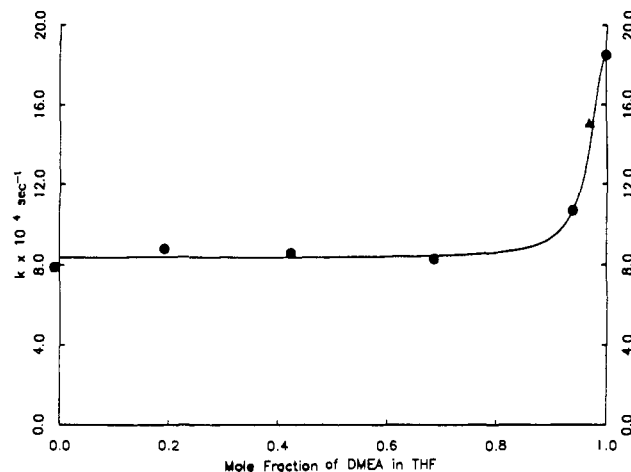


Figure 9. Pseudo-first-order rate constants for the metalation of imine **2-d₄** (0.004 M) by LDA (0.13 M) as a function of DMEA and THF composition. The units on the *x*-axis correspond to $[DMEA]/([DMEA] + [THF])$. An unweighted least-squares fit to eq 10 affords $K_{eq}(THF/DMEA) = 670 \pm 130$. The rate constant designated by a triangle (\blacktriangle) was not recorded under fully pseudo-first-order conditions and was not included in the fit.

observed in neat TMEDA vs neat THF results from a relative *destabilization* of TMEDA solvation in the LDA ground state that is attenuated in the transition state.

Figure 9 shows the measured pseudo-first-order rate constant for the metalation of imine **2-d₄** plotted as a function of DMEA mole fraction in THF. Fitting of the data to eq 10 ($S_1 = DMEA$ and $S_2 = THF$) affords $K_{eq}(THF/DMEA) = 670 \pm 130$ (favoring the THF solvate) and $k_{obsd}(DMEA)/k_{obsd}(THF) = 2$.³² This affords a ground-state energy difference, $\Delta G^\circ(C)$, of 3.6 ± 0.7 kcal/mol and transition-state energy difference, $\Delta G^\circ(D)$, of 2.9 ± 0.8 kcal/mol. Although the quality of the fits in both Figures 8 and 9 is reduced by the proximity of the fall-off region to the *y*-intercepts, the calculated values of $K_{eq}(THF/DMEA)$ confirm previous suggestions that THF is superior to DMEA as a ligand for LDA.¹⁰ The slightly higher rate observed in neat DMEA relative to neat THF is suggested to arise from a ground-state destabilization of the DMEA-solvated LDA that is relieved to only a limited extent in the transition state.

A plot of similar appearance is obtained for metalations of imine **6** in TMEDA/THF mixtures (Figure 10). This case is interesting because of the substantial (50-fold) difference in magnitude of the two *y*-intercepts. Nonetheless, Figure 10 serves only to provide a qualitative visual clarity since the solvent orders of the mechanisms operative at the two intercepts are different.

The relative solvent binding constants determined from TMEDA/THF and DMEA/THF mixtures reveal that THF is superior to either DMEA or TMEDA as ligands for LDA. One might also infer from the data that TMEDA is slightly better than DMEA. However, since the calculated values of K_{eq} are approximate, it would be imprudent to make subtle quantitative distinctions without confirmation. Accordingly, we measured the observed rate constants for metalation of **2-d₄** in TMEDA/DMEA mixtures over the entire mole fraction range (Figure 11). The gradual drift in Figure 11 is consistent with nearly equal affinities of TMEDA and DMEA for LDA. Least-squares analysis affords $K_{eq}(DMEA/TMEDA) = 5.5 \pm 1.6$ and $k_{obsd}(TMEDA)/k_{obsd}(DMEA) = 6$, which corresponds to $\Delta G^\circ(C) = 0.9 \pm 0.3$ (favoring DMEA in the ground state) and $\Delta G^\circ(D) = -0.07 \pm 0.02$ kcal/mol. (The small negative value denotes a reversal in stability, suggesting a slight preference for the TMEDA-solvated transition state.)

The rate data derived from the DMEA/TMEDA mixtures suggesting that DMEA is slightly better than TMEDA as a ligand for LDA dimer are not fully consistent with the data from DMEA/

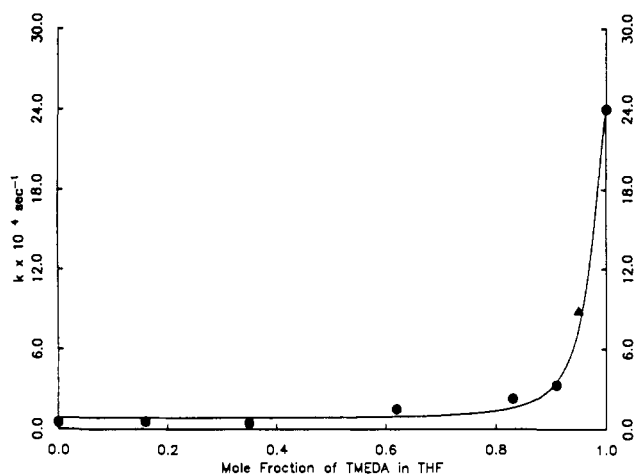


Figure 10. Pseudo-first-order rate constants for the metalation of imine **6** (0.004 M) by LDA (0.13 M) as a function of TMEDA and THF composition. The units on the x-axis correspond to $[TMEDA]/\{[TMEDA] + [THF]\}$. An unweighted least-squares fit to eq 10 affords $K_{eq}(THF/TMEDA) = 830 \pm 180$. (See text for caveat.) The rate constant designated by a triangle (\blacktriangle) was not recorded under fully pseudo-first-order conditions and was not included in the fit.

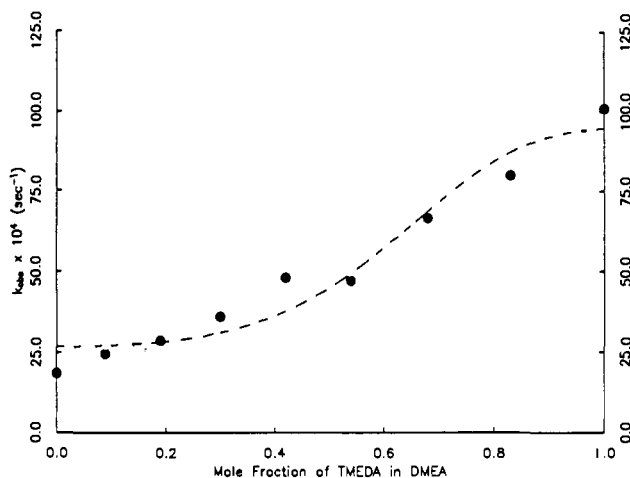


Figure 11. Pseudo-first-order rate constants for the metalation of imine **2-d₄** (0.004 M) by LDA (0.13 M) as a function of DMEA and TMEDA composition. The units on the x-axis correspond to $[TMEDA]/\{[DMEA] + [TMEDA]\}$. Each point corresponds to an average value of two independent measurements. The curve derives from an unweighted least-squares fit to eq 10 and affords $K_{eq}(DMEA/TMEDA) = 5.5 \pm 1.6$.

THF and TMEDA/THF mixtures. We view this as a prudent warning that the numerical values for the binding constants should not be interpreted literally.³³ The limited quality of fits may be a consequence of many factors noted above. Nevertheless, the qualitative relative binding constants are confirmed: $THF \gg TMEDA \approx DMEA$.

Discussion

We initiated studies of the imine metalations to determine the mechanistic basis of solvent- and substrate-dependent rates (Table I). We were interested secondarily in developing kinetic criteria for evaluating the effect of proximate ligating groups within a substrate on the reaction mechanism.

Summary of Imine Metalation Kinetics. Kinetic studies reveal that LDA-mediated metalations of various Schiff base derivatives can proceed by two distinctly different mechanisms. The *N,N*-dimethylhydrazones **i** and *N*-isopropylimines **ii** appear to be

(33) We note, for example, that $K_{eq}(THF/TMEDA) = 722 \pm 244$ using hydrazone **1** as the substrate. The apparent substrate dependence of $K_{eq}(THF/TMEDA)$ highlights the error inherent to the numerical fits.

metalated by isostructural monomer-based mechanisms irrespective of the donor solvent (Scheme I). Each manifests kinetic isotope effects of 6–11, fractional (0.5) LDA orders, and solvent-concentration-independent rates. They differ only in the absolute values of the pseudo-first-order rate constants. The assignment of TMEDA-solvated LDA dimer as bearing nonchelated (η^1 -bound) TMEDA ligands derives from a combination of crystallographic, spectroscopic, and computational studies described in detail previously.¹⁰ The putative transition structure (see precursor **iv**, Scheme I) bearing a nonchelating ligand originally was based upon kinetic studies showing that *N,N*-dimethylhydrazones metalations in DMEA—an isostructural analog of TMEDA incapable of bidentate coordination—follow the same rate profile as in TMEDA.¹⁰ We see the same relationship between DMEA and TMEDA for metalations of imines of general structure **ii**.

Rate studies of metalations of imines bearing pendant Me_2N moieties (**iii**) reveal some striking mechanistic details. Absolute rates and rate equations for metalations of **iii** in THF/hexane mixtures are qualitatively and quantitatively indistinguishable from their *N*-isopropyl counterparts (**ii**). In contrast, metalations in TMEDA and DMEA display first-order LDA dependencies and *inverse second-order donor solvent dependencies*, suggesting mechanisms involving rate-limiting metalation by *dimeric LDA dimer stripped free of donor solvents*. This pathway is strongly inhibited by addition of 2.5% THF, affording rates that are nearly indistinguishable from those measured in neat THF. Furthermore, metalations of **iii** in neat TMEDA or DMEA manifest substantial reductions in the measured isotope effects ($k_H/k_D = 2$ –3; Table II).

We offer the mechanism in Scheme II while deferring discussion of open dimer intermediate **v** to the next section. We do note that these rate studies provide the first experimentally verified example of a reaction of a lithium dialkylamide aggregate. Up to this point, aggregate-based reactivity had only been implicated by indirect, qualitative observations.³⁴ In fact, organolithium aggregate reactivity has been documented kinetically on only a few occasions to date.^{8–10,35}

Open Dimers in Organolithium Chemistry. To the best of our knowledge, the first hint of open dimer reactivity appeared in 1985. An ab initio calculation by Schleyer and co-workers implicated a favorable open-dimer-like transition state (but not intermediate) for addition of MeLi to formaldehyde.³⁶ In 1990, spectroscopic studies of a monomer–open dimer equilibrium of chiral cyclopentadienyllithiums were discussed in light of condition-dependent functionalization selectivities.³⁷ A subsequent report by Jackman and Rakiewicz suggested that an open dimer topology may be plausible for observable lithium phenolate mixed dimers.³⁸

The lithium dialkylamide open dimers emerged as putative reactive intermediates only recently, yet quite rapidly. Stable lithium dialkylamide open dimers first surfaced during the course of MNDO calculations of lithium dialkylamides by Romesberg and Collum.³⁹ Although the open dimers showed considerable stability, we (at least Collum) suspected them to be the result of a computational artifact. This notion was dispelled within several months when HMPA-solvated open dimer **10** was detected and

(34) Leading references: Hall, P.; Gilchrist, J. H.; Collum, D. B. *J. Am. Chem. Soc.* **1991**, *113*, 9571. See also ref 2.

(35) McGarrity, J. F.; Ogle, C. A.; Brich, Z.; Loosli, H.-R. *J. Am. Chem. Soc.* **1985**, *107*, 1810. Jackman, L. M.; Dunne, T. S. *J. Am. Chem. Soc.* **1985**, *107*, 2805. Jackman, L. M.; Rakiewicz, E. F.; Benesi, A. J. *J. Am. Chem. Soc.* **1991**, *113*, 4101.

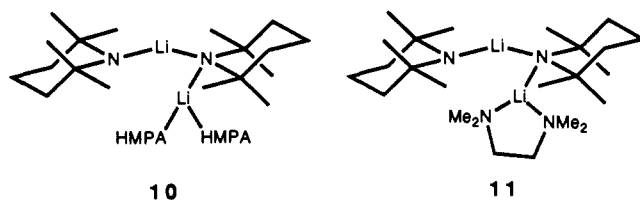
(36) Kaufmann, E.; Schleyer, P. v. R.; Houk, K. N.; Wu, Y.-D. *J. Am. Chem. Soc.* **1985**, *107*, 5560. A related calculation that includes open dimers as stable minima confirms the Schleyer–Houk conclusions: Nakamura, E.; Nakamura, M.; Koga, N.; Morokuma, K. Submitted for publication.

(37) Paquette, L. A.; Bauer, W.; Sivik, M. R.; Bühl, M.; Feigel, M.; Schleyer, P. v. R. *J. Am. Chem. Soc.* **1990**, *112*, 8776.

(38) Jackman, L. M.; Rakiewicz, E. F. *J. Am. Chem. Soc.* **1991**, *113*, 1202.

(39) Romesberg, F. E.; Collum, D. B. *J. Am. Chem. Soc.* **1992**, *114*, 2112.

fully characterized by NMR spectroscopy.^{40,41} In the manuscript describing the computational results we noted that "open dimers could provide a viable pathway for reaction of lithium amide dimers without intervening deaggregation."⁴² No direct evidence of LDA dimer reactivity was available at the time. Several interesting events took place immediately thereafter. The first was a double-blind experiment; Romesberg, Cajthaml, and Collum⁴³ calculated the structure of TMEDA-solvated open dimer **11** while Williard and Liu determined the structure of **11** by X-ray crystallography concurrently.⁴⁴ The two fully independent studies afforded nearly superimposable structures, differing only by a minor rotation about one N–Li bond. Interestingly, the calculations also strongly suggested that open dimers gain greater stabilization by the bidentate TMEDA interaction than do corresponding monomers. The second event was the emergence of the rate data described above that confirms direct dimer reactivity and led us to infer the intermediacy of open dimers.¹⁶ Several independent discussions of the consequences of R₂NLi–LiX mixed open dimers will appear in the foreseeable future.⁴⁵



The open dimer **v** depicted in Scheme II is not the only possible intermediate, yet it is strongly supported on the following grounds: (1) Intermediate **v** allows for the activation of the substrate by electrophilic catalysis.⁴⁶ The concomitant liberation of a reactive lone pair occurs without complete forfeiture of the stabilizing aggregation energy. (2) MNDO calculations clearly predicted that the internal lithiums of the dialkylamide open dimers will not retain a ligating solvent,³⁹ supporting the requisite dissociation of *both* donor solvents. (3) MNDO calculations on **11** and related open dimers predicted that chelation affords increased stability.⁴³ However, the efficiency of the open dimer metalation pathway stems from the *lability* of the DMEA and TMEDA ligands; if TMEDA had been a sufficiently strong ligand to afford open dimers as the *observable* species, the metalation would have been *inhibited* according to the principle of detailed balance.⁴⁷ (4) The internal proton abstraction via an eight-membered cyclic transition structure was initially suspicious; however, studies of related amine-based internal proton abstractions reveal eight-membered rings to be the *optimal* transition structure ring size.⁴⁸

(40) Romesberg, F. E.; Gilchrist, J. H.; Harrison, A. T.; Fuller, D. J.; Collum, D. B. *J. Am. Chem. Soc.* **1991**, *113*, 5751.

(41) For crystallographically characterized examples of lithium amide ladder structures showing open-dimer-like subunits, see: Armstrong, D. R.; Barr, D.; Clegg, W.; Hodgson, S. M.; Mulvey, R. E.; Reed, D.; Snaith, R.; Wright, D. S. *J. Am. Chem. Soc.* **1989**, *111*, 4719.

(42) Petasis and Teets recently invoked open dimer intermediates in a discussion of the selectivity of allenyl ketone metallations: Petasis, N. A.; Teets, K. A. *J. Am. Chem. Soc.* **1992**, *114*, 10328.

(43) Romesberg, F. E.; Cajthaml, C.; Collum, D. B. Unpublished.

(44) Williard, P. G.; Liu, Q.-Y. Unpublished.

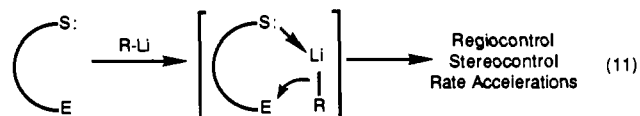
(45) Williard, P. G. *J. Am. Chem. Soc.* **1993**, *115*, 3380. Collum, D. B.; Romesberg, F. E. Manuscript in preparation.

(46) Jackman, L. M.; Dunne, T. S. *J. Am. Chem. Soc.* **1985**, *107*, 2805. Pierre, J.-L.; Handel, H. *Tetrahedron Lett.* **1974**, 2317. Loupy, A.; Seyden-Penne, J.; Tchoubar, B. *Tetrahedron Lett.* **1976**, 1677. Bunce, E.; Dunn, E. J.; Bannard, R. A. B.; Purdon, J. G. *J. Chem. Soc., Chem. Commun.* **1984**, 162. Chang, C. J.; Kiesel, R. F.; Hogen-Esch, T. L. *J. Am. Chem. Soc.* **1973**, *95*, 8446. Loupy, A.; Seyden-Penne, J. *Tetrahedron* **1980**, *36*, 1937.

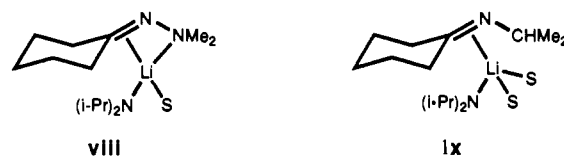
(47) Casado, J.; Lopez-Quintela, M. A.; Lorenzo-Barral, F. M. *J. Chem. Educ.* **1986**, *63*, 450. Hammes, G. G. *Principles of Chemical Kinetics*; Academic Press: New York, 1978; pp 14,15.

(48) McManus, S. P.; Capon, B. *Neighboring Group Participation*; Plenum Press: New York, 1976, p 58. See also: Bernardi, A.; Capelli, A. M.; Cassinari, A.; Comotti, A.; Gennari, C.; Scolastico, C. *J. Org. Chem.* **1992**, *57*, 7029. Bernardi, F.; Bongini, A.; Cainelli, G.; Robb, M.; Valli, G. S. *J. Org. Chem.* **1993**, *58*, 750.

Complex-Induced Proximity Effects: Kinetic Criteria. Beak and Meyers coined the term "complex-induced proximity effect" (CIPE) to describe those instances in which reagent-substrate precomplexation facilitates the subsequent reaction with a proximate electrophilic moiety (eq 11).^{11,12} CIPEs and synonymous chelation-directed organometallic reactions (Cram chelation model)¹⁴ are discussed extensively throughout the organometallic literature.¹⁵ CIPEs are usually evidenced by reaction rates and selectivities that differ from those observed with the internal ligands absent. Unfortunately, these criteria do not exclude other steric and inductive effects, often precluding a clear demonstration of a discrete metal–ligand interaction.



One of the original goals of this study was to develop a kinetic method for documenting the existence of a CIPE. The essential features of our premise can be illustrated with the comparison of *N,N*-dimethylhydrazones and the isostructural *N*-isopropylimines. In light of kinetic studies we previously argued species **viii** bearing a hydrazone functioning as four-electron donor was a logical intermediate en route to the rate-limiting metalation transition state.¹⁰ The supposition was appealing in light of Bergbreiter's studies revealing nearly equal propensities to metalate *syn* and *anti* to the Me₂N moiety.^{49,50} Since only the stoichiometry of the transition state had been determined, the Me₂N–Li π interaction was speculative. However, we surmised that if the Me₂N–Li interaction was both real and *obligatory*, then metallations of the isostructural imines would be forced to proceed through intermediate **ix** bearing an additional donor solvent incorporated from the medium in place of the Me₂N moiety. The requisite external solvation should cause a precipitous decrease in the metalation rates for *N*-isopropylimines and would be manifested by a *fundamental change in the mathematical form of the rate equation as reflected in the solvent order*. While significantly lower metalation rates were observed for the *N*-isopropylimines (Table I), the rate equations for *N*-isopropylimines and *N,N*-dimethylhydrazones are indistinguishable in every respect, including zero solvent orders. Consequently, we find no direct evidence supporting a discrete Me₂N–Li interaction in the hydrazone metalation transition state. Although we cannot exclude a *non-obligatory* lithium solvation by the Me₂N group as the source of the greater hydrazone metalation rates, looking beyond simple inductive effects would defy Ockham's razor.^{51,52}



The results for imines of type **iii** provide support for a CIPE that is nearly unequivocal. By placing the Me₂N moiety remotely on the *N*-isopropyl fragment, the ill-defined inductive and steric

(49) Ludwig, J. W.; Newcomb, M.; Bergbreiter, D. E. *J. Org. Chem.* **1980**, *45*, 4666.

(50) For general reviews on the chemistry of lithiated imines, see: Bergbreiter, D. E.; Momongan, M. In *Comprehensive Organic Synthesis*; Trost, B. M., Fleming, I., Eds.; Pergamon: New York, 1989; Vol. 1, p 503. Martin, S. F. *Ibid.* Vol. 1, p 475. Hickmott, P. W. *Tetrahedron* **1982**, *38*, 1975. Enders, D. In *Current Trends in Organic Synthesis*; Nozaki, H., Ed.; Pergamon: New York, 1983. Whitesell, J. K.; Whitesell, M. A. *Synthesis* **1983**, 517. Fraser, R. R. In *Comprehensive Carbanion Chemistry*; Bunce, E., Durst, T., Eds.; Elsevier: New York, 1980.

(51) "Plurality should not be assumed without necessity". Adams, M. M. *William Ockham*; University of Notre Dame Press: Notre Dame, 1987; p 156.

(52) Collum, D. B. *Acc. Chem. Res.* **1992**, *25*, 448.

effects would be minimized. In the absence of a CIPE one would expect both the rate equation and absolute reaction rates to coincide with those observed for the simple *N*-isopropyl derivatives. Indeed, the rates and rate equations for metalations of ii and iii in THF/pentane mixtures were essentially indistinguishable, affording strong negative evidence refuting a CIPE. Metalations of ii and iii in trialkylamine solvent, on the other hand, follow different rate equations; ii appears to metalate by a monomer-based mechanism (Scheme I), while iii appears to metalate via a dimer-based mechanism (Scheme II). Also, the emergence of the dimer pathway is accompanied by substantial rate increases. For example, the absolute metalation rates of iii are >10 times higher in neat DMEA or TMEDA than in THF, and they increase exponentially upon reducing the [DMEA] or [TMEDA] to 35% by volume. (The metalations become too fast to monitor at lower R_3N concentrations.) Most significant, however, is that the pronounced changes in the rate equations resulting from introduction of a ligand into the substrate establish the existence of a CIPE beyond a reasonable doubt.^{12,13}

On the Role of TMEDA as a Donor Ligand. Although previous spectroscopic and kinetic studies provided indirect evidence that THF is substantially better than TMEDA as a ligand for LDA, a quantitative measure of their relative donorities was elusive.¹⁰ The apparently poor solvating properties of TMEDA and the failure of the metal–ligand bond strength to correlate with observed reactivity prompted us to review the structural and mechanistic literature of TMEDA.⁵² Quite surprisingly, we found the notion that TMEDA is a strong ligand for lithium to be poorly founded. Among the many hypotheses offered in the review, the following are especially pertinent to this discussion: (1) An *inverse* correlation between metal–ligand bond strength and reactivity may be more logical than the often-cited direct correlation. (2) Many of the spectacular rate effects of TMEDA that have helped shape our ideas about structure–reactivity relationships within organolithium chemistry can be interpreted in the context of a weak (rather than strong) TMEDA–Li interaction. (3) Monomers are not necessarily more reactive than the corresponding aggregates.

The kinetics of imine metalations reinforce these points. The exponential rate increases observed upon decreasing the TMEDA or DMEA concentrations provide excellent support for the contention⁵² that other TMEDA-based rate accelerations may stem from the *lability* of the TMEDA–Li linkage. Although we cannot ascertain the relative stabilities of transiently formed monomers (iv, Scheme I) and open dimers (v, Scheme II), the open-dimer-based pathway is considerably more efficient under judiciously chosen conditions. In light of our preconception that chelation generally promotes reactions through monomers, we find it ironic that the dimer-based metalation pathway emerged from metalation rate studies in which both the substrate and donor solvent are potential chelators.

We described a method by which the *kinetics* of metalation could provide a semiquantitative method for determining the thermodynamics of solvation. In turn, this allows us to dissect observed relative rate constants into the separate contributions of ground-state and transition-state energy differences. As a result of the different inherent reactivities of intermediates vi and vii (Scheme IV), a plot of k_{obsd} vs mole fraction of two solvents, S_1 and S_2 , affords a sigmoidal function (Figure 6). The two y -intercepts are the limiting rate constants for metalations by vi and vii with corresponding activation energies $\Delta G^\circ(A)$ and $\Delta G^\circ(B)$ (Figure 7). The location of the fall-off region (the inflection point) affords the relative solvent binding constants and, in turn, the stabilities of ground-state structures vi and vii ($\Delta G^\circ(C)$ in Figure 7). Overall, plots of k_{obsd} vs donor solvent composition (Figure 6) provide the relative ground-state stabilities and transition-state stabilities ($\Delta G^\circ(C)$ and $\Delta G^\circ(D)$ in Figure 7) essential to even the most rudimentary understanding of the

observed relative rate constants. We can summarize the results as follows: (1) THF shows a greater affinity for LDA (1–2 kcal/mol *per solvent*) than does either TMEDA or DMEA. (2) The binding constants for TMEDA and DMEA are nearly equal, providing further support for the assignment of an η^1 -solvated TMEDA in both the ground state and the rate-limiting transition state. (3) High rates observed for metalations of imine ii in TMEDA and DMEA (relative to THF) stem from ground-state destabilizations that are partially relieved in the rate-limiting transition states. (4) The substantially greater rates for metalation of imines of type iii in trialkylamines (TMEDA or DMEA) relative to THF stem from substantial ground-state destabilizations that are relieved to a considerable extent upon double solvent dissociation. While specific features of the imine metalations as well as certain approximations facilitated the analysis (see Results), we feel that the strategy may be generalizable to other solvents and to other classes of organolithium reagents and reactions.

Conclusion

Through systematic investigations of the mechanisms by which LDA metalates hydrazones and related imines we are beginning to understand the mechanistic underpinnings of solvent- and substrate-dependent reactivities. The work reveals insights into the relationships of solvation, aggregation, and reactivity that apply to other areas of organolithium chemistry as well. Some specific conclusions and insights include the following:

1. We provided direct kinetic evidence that lithium diisopropylamide can react as either monomers or dimers, depending on the precise choice of substrate and solvent. The evidence for open dimer intermediates in the dimer-based pathway seems to be quite compelling. The remarkable double donor solvent dissociation results in an inverse correlation of reaction rate with solvent donority and concentration. Treating lithium ion solvation as discrete metal–ligand interactions manifesting discrete terms in kinetic rate equations can be quite revealing.

2. It is suggested that complex-induced proximity effects (CIPEs) may be most convincingly detected at the level of the rate equation. A change in the rate equation resulting from introduction of an internal ligating group provides strong evidence of a CIPE, whereas the absence of such a change provides less compelling evidence refuting a CIPE.

3. A method for obtaining semiquantitative data pertaining to the relative propensities of standard donor solvents to bind to LDA is described. The insight into LDA ground-state stability facilitates discussions of relative reactivities. The high kinetic reactivity resulting from the lability of the TMEDA–LDA linkage supports previous contentions⁵² that at least some TMEDA-mediated rate accelerations may stem from pronounced ground-state destabilization rather than from transition state stabilization.

4. Probably the most generally important conclusion comes in the form of a reminder that relative reaction rates cannot possibly provide significant mechanistic insight without at least a rudimentary knowledge of the structures and stabilities of both the ground states and the transition states. Curiously, it is often the ground-state stabilities that are omitted from implicitly thermochemical arguments.

Experimental Section

Reagents and Solvents. THF, dimethylethylamine (DMEA), TMEDA, and all hydrocarbons were distilled by vacuum transfer from blue or purple solutions containing sodium benzophenone ketyl. The hydrocarbon stills contained 1% tetraglyme to dissolve the ketyl. The LDA was prepared as a solid from *n*-BuLi (Aldrich) and purified by the standard literature procedure.¹⁹ The diphenylacetic acid used to check solution titers⁵³ was recrystallized from methanol and sublimed at 120 °C under full vacuum.

Air and moisture sensitive materials were manipulated under argon or nitrogen using standard glovebox, vacuum line, and syringe techniques.

Kinetics. The apparatus and flow system for following the kinetics of metalation of imines have been described previously.¹⁰ Helium was used as the inert atmosphere to minimize a degassing problem in the flow system. Automated data collection allowed the typical rate constant to be determined from 150–300 independent absorbance measurements over ≥ 6 half-lives. The measured rate constants depend minimally on the choice of frequency to establish the spectral base line; 1710 cm^{-1} was found to minimize random scatter and give the most reproducible results. All other aspects of the kinetic and statistical analyses were carried out as described previously.¹⁰ Other pertinent details are found in Results.

Substrates. The imines were prepared by standard literature procedures modified to ensure successful preparations of the deuterated derivatives without label washout. The deuterated imines were prepared from the corresponding deuterated ammonium salts and deuterated ketones¹⁷ following the representative procedure described below. The deuterated amine hydrochlorides (RND_3Cl) used in the protocol were prepared by (1) precipitating the hydrochloride salt (RNH_3Cl) from anhydrous diethyl ether at 0 °C with HCl gas and (2) successively dissolving the salt in D_2O (0.75 mL/g) with evaporation under vacuum (six to eight iterations).

2,2,6,6-Tetrauteriocyclohexanone, *N*-Isopropylimine (2- d_4). To a dry 25-mL round bottom flask containing 500 mg of deuterated, activated 4-Å molecular sieves and a stir bar were added *i*-PrND₃Cl (2.0 g, 20 mmol), 2,2,6,6-tetrauteriocyclohexanone¹⁷ (2.0 g, 20 mmol), and Proton Sponge (8.6 g, 40 mmol). To this mixture was added 5 mL of anhydrous triethylamine under a purge of nitrogen gas. The flask was sealed with a two-way ground-glass stopcock, secured by a clamp and wire, and heated at ~ 100 °C overnight. Distillation at full vacuum (0.01 mm, bp = 27–28 °C) afforded imine 2- d_4 (1.5 g, 47% yield) as a clear, colorless oil that displays moisture and light sensitivity: $^{13}\text{C}\{^1\text{H}\}$ NMR (100 MHz, CDCl_3) δ 23.9, 26.1, 26.8, 27.2, 27.6, 39.8 (quint, $J_{\text{C,D}} = 19$ Hz), 48.8,

170.5; ^1H NMR (400 MHz, CDCl_3) δ 1.06 (d, $J = 6.4$ Hz, 6 H), 1.58 (m, 2 H), 1.66 (m, 4 H), 2.19 (t, $J = 6.8$ Hz, 2 H, missing when fully deuterated), 2.23 (t, $J = 5.2$ Hz, 2 H, missing when fully deuterated), 3.63 (m, $J = 6.4$ Hz, 1 H); IR 1660 cm^{-1} (C=N–R).

2-Methylcyclohexanone- d_3 , (2-dimethylamino-1-methyl)ethylimine (6- d_3). $^{13}\text{C}\{^1\text{H}\}$ NMR (100 MHz, CDCl_3) δ 17.4, 20.3, 23.7, 27.6, 27.8, 35.2 (quint, $J_{\text{C,D}} = 18$ Hz), 44.3 (t, $J_{\text{C,D}} = 19$ Hz), 46.2, 52.2, 67.0, 173.5; ^1H NMR (200 MHz, CDCl_3) δ 1.05 (d, $J = 6.2$ Hz, 3 H), 1.08 (d, $J = 5.6$ Hz, 3 H, splitting disappears when fully deuterated), 1.64 (m, 6 H), 2.12 (m, 3 H, missing when deuterated), 2.20 (s, 6 H), 2.31 (d, $J = 6$ Hz, 2 H), 3.65 (m, 1 H); IR 1659 cm^{-1} C=N–R.

2-Methylcyclohexanone- d_3 , *N*-Isopropylimine (5- d_3). $^{13}\text{C}\{^1\text{H}\}$ NMR (100 MHz, CDCl_3) δ 17.5, 23.3, 23.9, 26.7, 27.7, 35.1 (quint, $J_{\text{C,D}} = 19$ Hz), 41.9 (t, $J_{\text{C,D}} = 19$ Hz), 48.7, 172.4; ^1H NMR (400 MHz, CDCl_3) δ 1.05 (d, $J = 6.0$ Hz, 6 H), 1.08 (d, $J = 5.7$ Hz, 3 H, splitting disappears when deuterated), 1.6 (m, 2 H), 2.15 (m, 4 H), 2.35 (m, 3 H, missing when fully deuterated), 3.67 (m, 1 H); IR 1659 cm^{-1} C=N–R.

Acknowledgment. We thank the National Institutes of Health for direct support of this work. We also acknowledge the National Science Foundation Instrumentation Program (CHE 7904825 and PCM 8018643), the National Institutes of Health (RR02002), and IBM for support of the Cornell Nuclear Magnetic Resonance Facility. We thank Andrew Streitwieser, James Krom, Floyd Romesberg, Brett Lucht, and Barry K. Carpenter for help and advice.

Supplementary Material Available: Tables of rate constants, additional kinetic plots, and derivations of eqs 7 and 10 (16 pages). Ordering information is given on any current masthead page.